

Fractional charges and spin-charge separation in one-dimensional Wigner lattices

M. Daghofer and P. Horsch

Max-Planck-Institut für Festkörperforschung, Heisenbergstrasse 1, D-70569 Stuttgart, Germany

(Dated: May 25, 2019)

We study density response $N(k, \omega)$ and one-particle spectra $A(k, \omega)$ for a Wigner lattice model at quarter filling using exact diagonalization. These spectra clearly indicate that an electron decays into a pair of interacting domain walls and a spinon. Domain-wall interaction, controlled by fractional charges, manifests itself in an antibound quasi-particle in $A(k, \omega)$, in striking contrast to a bound exciton in $N(k, \omega)$. We present a case of extreme particle-hole asymmetry, where photoemission shows spin-charge separation, while inverse photoemission exhibits uncorrelated one-particle bands. Inclusion of the spin reduces the stability region of the Wigner crystal in the phase diagram.

PACS numbers: 71.10.Pm, 73.20.Qt, 78.20.Bh

In contrast to higher dimensions, where interacting electrons are renormalized into ‘Landau quasi-particles’ that near the Fermi surface still ‘look’ like electrons, drastic things can happen in one dimension [1]. The elementary excitations are collective ones involving many electrons, *spin and charge separate* and move independently of each other, as seen, e.g., in photoemission (PES) experiments [2]. Another case where many-body effects lead to an apparent splitting of elementary particles is *quantum number fractionalization* [3]. Probably its most famous realization is the fractional quantum Hall effect [4]. Likewise, Peierls distorted [5] and charge-ordered [6, 7] one-dimensional (1D) systems with degenerate ground states have fractionally charged solitons or domain walls as elementary excitations. In fact, quantum number fractionalization in one and two dimensions are intimately related [8]. This Letter presents a first study of dynamic observables for a model showing both effects, spin-charge separation as well as quantum number fractionalization.

When (long-range) Coulomb interaction is the dominant energy scale of a system, electrons try to minimize their energy by maximizing their distance and crystallize into a Wigner lattice (WL) [9]. Hubbard suggested this mechanism in the context of TCNQ charge-transfer salts [6] where it is, however, difficult to distinguish from a $4k_F$ charge-density wave (CDW) driven by a Fermi surface instability [6, 7, 10]. As pointed out recently [11], longer-range hopping changes the Fermi-surface topology in doped edge-sharing CuO-chain compounds like $\text{Na}_{1+x}\text{CuO}_2$ [12] and $\text{Ca}_{2+y}\text{Y}_{2-y}\text{Cu}_5\text{O}_{10}$ [13], and this allows a clear distinction between the Fermi-surface independent WL and the CDW.

The elementary excitations of a WL consist of domain walls (DWs). Their fractional charge follows from topological arguments [6, 7, 14] and merely reflects the n -fold ground-state degeneracy at $x = m/n$ filling – it is not related to the specific form of the interaction that generates the charge order. In this Letter, we show that these charges have direct physical meaning in a model with long-range Coulomb repulsion among electrons, because the resulting effective interaction between DWs is also

Coulomb-like with a coupling constant determined by the fractional charges, their signs and distance. Consistent with the formal charges, the interaction is *attractive* for the charge response [15, 16] but *repulsive* for the electron addition (removal) process, leading to a straightforward interpretation of coherent signals in the respective spectra $N(k, \omega)$ and $A(k, \omega)$ as bound and antibound states. The correspondence is tied to the long-range nature of Coulomb repulsion and is absent for models with truncated interactions.

As the energy scale for spin excitations is much smaller than either the Coulomb repulsion or the kinetic energy, previous investigations considered WL formation of spinless fermions. Here, we will address the impact of the spin degree of freedom and shall see that it offers an additional channel that weakens WL charge order regardless of its energy scale. This effect results solely from the fact that electrons with different spin can be distinguished while electrons with the same spin cannot. We show further how the interplay of spin and DW excitations leads to two different scenarios for the spectral density: (i) For nearest neighbor hopping, the coherent antibound DW excitation undergoes spin-charge separation in perfect analogy to an electron or hole added to the half-filled 1D Hubbard model. (ii) For 2nd neighbor hopping, we find striking differences between the particle and hole channels, where an electron behaves like an independent particle while a hole decays into a spinon and a holon.

We study the Hubbard-Wigner Hamiltonian [15]

$$H = t_1 \sum_{i,\sigma} (c_{i,\sigma}^\dagger c_{i+1,\sigma} + \text{h.c.}) + t_2 \sum_{i,\sigma} (c_{i,\sigma}^\dagger c_{i+2,\sigma} + \text{h.c.}) + U \sum_i n_{i,\uparrow} n_{i,\downarrow} + \sum_{l=1}^{l_{\max}} V_l \sum_i (n_i - \bar{n})(n_{i+l} - \bar{n}), \quad (1)$$

with nearest neighbor (NN) and next nearest neighbor (NNN) hopping amplitudes t_1 and t_2 . Operator $c_{i,\sigma}^\dagger$ ($c_{i,\sigma}$) creates (destroys) an electron with spin σ at site i , $n_{i,\sigma} = c_{i,\sigma}^\dagger c_{i,\sigma}$ and $n_i = n_{i,\uparrow} + n_{i,\downarrow}$ give the density, \bar{n} is

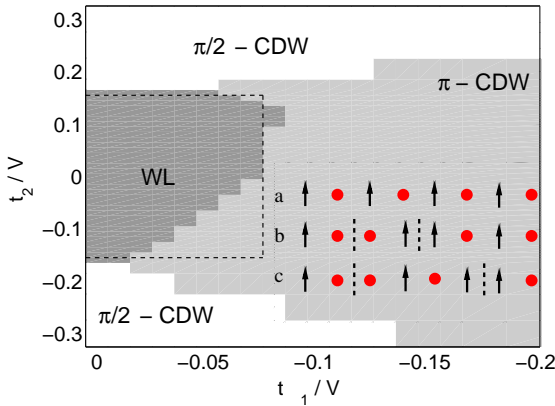


FIG. 1: Phase diagram inferred from the charge-structure factor for $L = 12$, $U = 4V$. Dark gray: Wigner lattice (WL) with periodicity π , light gray: CDW with periodicity π (π -CDW), white: CDW with periodicity $\pi/2$ ($\pi/2$ -CDW). The dashed lines give the phase boundaries for the spinless case. The arrows (circles) represent electrons (holes) for (a) the perfect WL, (b) one displaced electron leading to two DWs indicated by dashed lines, that can move via NN hopping t_1 (c).

the average density. We focus on long-range Coulomb repulsion $V_l = V/l$ [17], but also discuss truncated interaction ($l_{\max} = 3$) to illustrate that truncation has a strong impact on the excitation spectra. The NN Coulomb matrix element V is used as unit of energy. We treat chains up to $L = 20$ in the spinless case and $L = 16$ with spin using Lanczos diagonalization; we investigate quarter filling, i.e., one electron per two sites.

We analyze the charge structure factor $N(q) = \langle \rho_{-q} \rho_q \rangle$, with $\rho_q = 2/L \sum_r \exp(-iqr) n_r$ to determine the phase diagram Fig. 1. Without hopping ($t_1 = t_2 = 0$), the ground state of (1) is given by the perfectly charge-ordered WL with one electron on every other site. Such order frustrates NNN hopping t_2 , and the system therefore prefers to break the WL at large t_2 in order to gain kinetic energy. This leads to a CDW with periodicity $\pi/2$. NN hopping t_1 , on the other hand, is not frustrated in the WL and can induce charge fluctuations. When the WL starts to melt with growing t_1 , the lowest-energy (and hence most important) fluctuations have two DWs, one consisting of two electrons next to each other and the other of two holes [15, 16], see the schematic illustration in Fig. 1. The fluctuations preserve periodicity π , but weaken charge order and lead to a gradual crossover from the WL to a CDW with periodicity π [15]. The crossover line in Fig. 1 is given by the points where $N(q)$ at $q = \pi$ drops below 0.8, this coincides roughly with the inflection point of $N(\pi)$ vs. t_1 .

Figure 1 shows the phase diagram both for electrons with spin (gray shades) and for spinless fermions (dashed lines) and reveals a marked difference for t_1 and t_2 both negative: While the crossover from the WL to the π -CDW is driven exclusively by t_1 in the spinless case, it

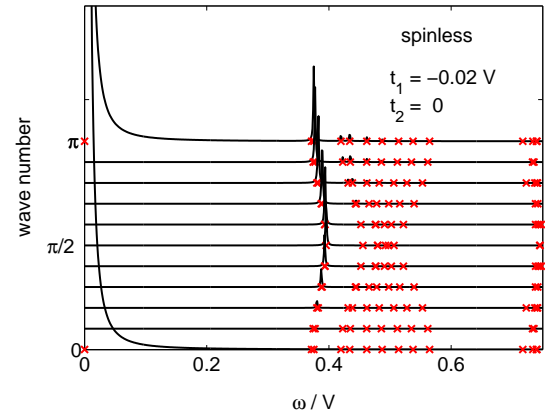


FIG. 2: (Color online) Density response $N(q, \omega)$ with $t_1 = -0.02V$ and $t_2 = 0$. The \times show the eigen energies.

depends on both t_1 and t_2 in the model with spin (i.e., t_2 helps to destabilize charge order). U has very little impact on the crossover and this means that the difference to the spinless model is not caused by (virtual) double occupancies or by superexchange $\sim J_2 = 4t_2^2/U$; it can instead be understood by analyzing the *dynamics of DWs*. As illustrated in Fig. 1, DWs can move via NN t_1 -hopping [15, 16], with and without spin. Concerning NNN hopping in the spinless case, it can be shown that t_2 -processes directed to the right (i.e. from site i to $i+2$) and to the left (from $i+2$ to i) obtain a relative Fermi sign and cancel exactly. t_2 can therefore not affect the states most relevant for the ground state [18], neither the WL (because of frustration, see above) nor the two-DW component (because of cancellation), and does thus not influence the crossover. For electrons with spin, however, the states produced by right-moving processes do not have the same sequence of up- and down-spins as those from left-moving ones. NNN hopping therefore does not cancel and instead lowers the energy of the two-DW states, this enhances their contribution to the ground state and consequently weakens charge order. The effect of spin results thus solely from symmetry and does not depend on coupling constants or on the energy scale of spin excitations.

The relevance of DWs becomes even clearer in the case of the dynamic charge structure factor

$$N(q, \omega) = \sum_m |\langle m | \rho_q | \phi_0 \rangle|^2 \delta(\omega - (E_m - E_0)), \quad (2)$$

where $|m\rangle$ and E_m are the eigenstates and energies of the Hamiltonian, and $|\phi_0\rangle$ is the ground state with energy E_0 . For the perfect WL without quantum fluctuations, it shows only signals at $\omega = 0$ and momenta $k = \pi$ and $k = 0$. Finite-frequency signals are produced by fluctuations around perfect charge order, i.e., by states with at least two DWs. DWs can move by t_1 and feel an attractive potential, which can be interpreted as Coulomb

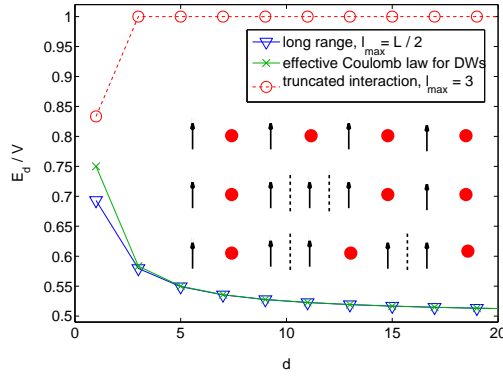


FIG. 3: (Color online) Potential E_d between two domain walls at distance d for long-range electron-electron interaction ($l_{\max} = L/2$, ∇), effective Coulomb law $E_d = 1/2 + e^2/(4d)$ (\times), and for truncated electron-electron interaction ($l_{\max} = 3$, \circ). The schematic configurations (symbols as in Fig. 1) show two DWs created by adding a particle to the WL and their movement via NN hopping.

attraction between charges $\pm e/2$ of opposite sign and half the magnitude of electron charge. This potential leads to an exciton below a two-DW continuum [15], and Fig. 2 reveals that most spectral weight is observed in this exciton, while the two-DW continuum at $0.4V \lesssim \omega \lesssim 0.6V$ contains almost none.

The effective DW interaction continues to correspond to their formal fractional charges when an electron is added to (or removed from) the WL. The schematic illustration in Fig. 3 shows that an additional electron creates two DWs. Both DWs consist of electron pairs with formal charge $-e/2$ each. Their interaction E_d at distance d can be obtained by calculating the potential energy for a configuration where the DWs (i.e., the dashed lines in the configurations depicted in Fig. 3) are d sites apart, the resulting *repulsive* interaction is denoted by ∇ in the main panel of Fig. 3. An excellent approximation for $d > 1$ is given by $1/2 + e^2/(4d)$, i.e., by a Coulomb law acting on two charges of $-e/2$ (\times in Fig. 3). The formal charges therefore have a very direct physical meaning, which is completely absent from a model with truncated electron-electron interaction ($l_{\max} = 3$): In this case, the effective DW potential is short-range and *attractive* (\circ in Fig. 3). This means that the effective DW charges determining the interaction have the ‘wrong’ sign for a truncated interaction when compared to the formal charges.

The impact of these potentials can be observed in the one-particle spectral density

$$A(k, \omega) = \sum_m |\langle m^+ | c_{k,\uparrow}^\dagger | \phi_0 \rangle|^2 \delta(\omega - (E_m^+ - E_0)) + \sum_m |\langle m^- | c_{k,\uparrow} | \phi_0 \rangle|^2 \delta(\omega - (E_m^- - E_0)), \quad (3)$$

where $|m^+\rangle$ ($|m^-\rangle$) are eigenstates with eigenenergies E_m^+ (E_m^-) of the Hamiltonian with one particle added (re-

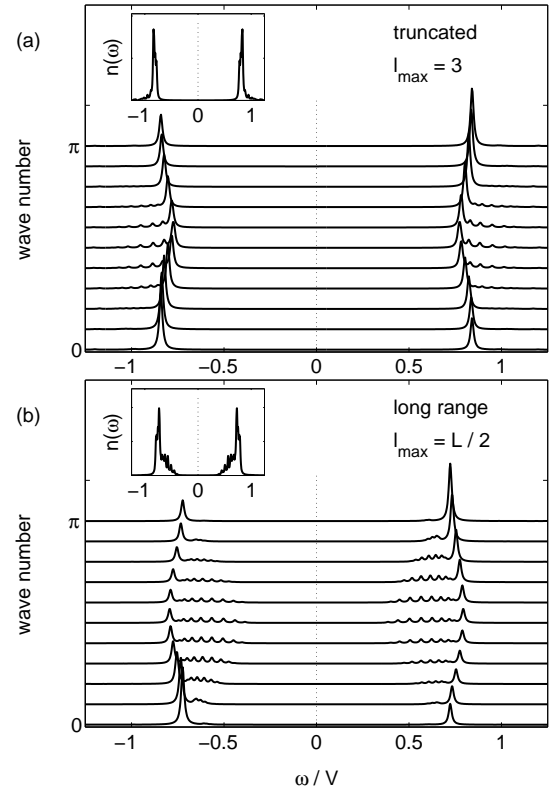


FIG. 4: Spectral density $A(k, \omega)$ for spinless fermions for (a) truncated V_i and (b) long-range V_i with $t_1 = -0.05V, t_2 = 0$. Insets show the density of states.

moved). For the situation of a spinless fermion added to the perfect WL, a simplified Hamiltonian in terms of DWs can be obtained that contains hopping t_1 and the potential energy E_d . By assuming a simplified DW potential $E_d = E_1$ for $d = 1$ and $E_d = E_\infty$ for $d > 1$ [19], we obtain $A(k, \omega)$ by a procedure similar to that used in Ref. 15 for the exciton. We find that inverse photoemission (IPES) for momentum k consists of (i) an incoherent two-DW continuum $E_\infty - 4t_1 \sin k < \omega < E_\infty + 4t_1 \sin k$, and (ii) a coherent quasiparticle with dispersion

$$\epsilon(k) = E_1 + \frac{(2t_1 \sin k)^2}{E_1 - E_\infty}. \quad (4)$$

Our calculation also shows that the continuum has larger weight at the edge close to the quasiparticle and very low weight at the other side. Equation (4) shows that the quasiparticle energy depends on $E_1 - E_\infty$: For a truncated interaction ($l_{\max} = 3$), which induces DW attraction $E_1 < E_\infty$ (see Fig. 3), the collective excitation is below the continuum. In contrast, it is above in the long-range case with DW repulsion $E_1 > E_\infty$. The spectra obtained by exact diagonalization of the spinless electron Hamiltonian (1) are shown in Fig. 4. In perfect accordance with the DW analysis, the quasiparticle lies below the continuum for $l_{\max} = 3$ (Fig. 4(a)), but above it for $l_{\max} = L/2$ (Fig. 4(b)). Hence, this unusual antibound

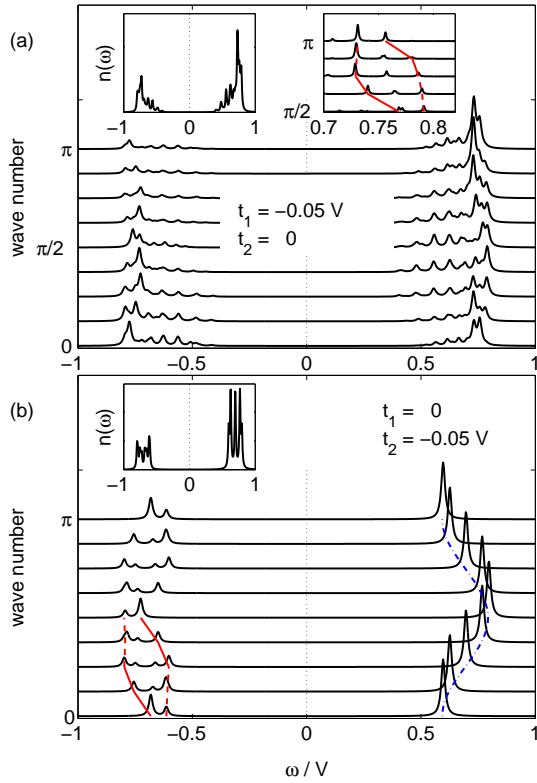


FIG. 5: (Color online) Spectral density $A(k, \omega)$ with spin for (a) $t_1 = -0.05V, t_2 = 0$, (b) $t_1 = 0, t_2 = -0.05V$, $U = 4V$, $L = 16$. Insets on the left show the density of states. In (a), the right-hand inset shows a blow-up of IPES with a higher energy-resolution, the dashed and solid lines indicate spinon and ‘anti-holon’ branches (guides to the eye). In (b), spinon and holon branches in PES are indicated by dashed and solid lines (guides to the eye), the dash-dotted line in IPES gives the one-particle dispersion $E(k) = V \ln 2 + 2t_2 \cos 2k$.

state results from the long-range nature of Coulomb repulsion.

Having understood the dynamics of the spinless system, i.e., of the charge sector, we now include the spin. An inserted electron or hole then produces a spin in addition to the two DWs giving the charge dynamics. Remarkably, one can interpret the results in a similar manner as for a hole in the half-filled Hubbard model, despite the much more complex charge sector: The spectral density depicted in Fig. 5(a) reveals that the antibound quasiparticle of the spinless model changes into a convolution of spinon and ‘anti-holon’ branches in the model with spin. (Note the inset on the right showing a blow-up of IPES with higher energy-resolution.) In the present case, the ‘anti-holon’ is given by the antibound 2-DW state that is the elementary collective excitation of the charge sector.

Motivated by experimental data indicating that NNN hopping t_2 is larger than t_1 in $\text{Na}_3\text{Cu}_2\text{O}_4$ [11], we now turn to the spectral density for $t_2 \neq 0$, choosing $t_1 = 0$

for simplicity. The ground state is then given by the perfectly charge ordered WL, an electron added in IPES goes into an empty site and can move freely on the empty sublattice, without any interaction with the occupied sublattice (as $t_1 = 0$). Consequently, IPES shows a one-particle-like tight-binding band with dispersion $E(k) = V \ln 2 + 2t_2 \cos 2k$, see $\omega > 0$ in Fig. 5(b). The situation for a hole is, however, completely different: The hole goes into the occupied sublattice, which is a *Hubbard* chain, and it therefore undergoes spin-charge separation. The resulting spinon and holon branches in PES can be seen for $\omega < 0$ in Fig. 5(b). Surprisingly, one and the same observable, the spectral density, can show both pure one-particle behavior (in the particle sector) and strongly correlated behavior (in the hole sector).

To conclude, we have investigated a quarter-filled Hubbard-Wigner model appropriate for edge-sharing $\text{Na}_3\text{Cu}_2\text{O}_4$, and find that electrons decay into a spinon and two domain walls. We have shown that this decay is seen in dynamic observables and that its signatures include unusual and novel features: For example, an antibound quasiparticle undergoes spin-charge separation, and the spectral density exhibits dramatic particle-hole asymmetry - an electron behaves as an independent particle while a hole decomposes into spinon and holon.

We thank A. M. Oleś for careful reading of the manuscript and for helpful suggestions.

- [1] S. Maekawa and T. Tohyama, *Rep. Prog. Phys.* **64**, 383 (2001).
- [2] B. J. Kim *et al.*, *Nature Physics* **2**, 397 (2006).
- [3] M. Oshikawa and T. Senthil, *Phys. Rev. Lett.* **96**, 060601 (2006).
- [4] R. B. Laughlin, *Phys. Rev. Lett.* **50**, 1395 (1983).
- [5] A. J. Heeger *et al.*, *Rev. Mod. Phys.* **60**, 781 (1988).
- [6] J. Hubbard, *Phys. Rev. B* **17**, 494 (1978).
- [7] M. J. Rice and E. J. Mele, *Phys. Rev. B* **25**, 1339 (1982).
- [8] A. Seidel and D.-H. Lee, *cond-mat/0604465* (2006).
- [9] E. Wigner, *Phys. Rev.* **46**, 1002 (1934).
- [10] F. Nad and P. Monceau, *J. Phys. Soc. Jpn.* **75**, 051005 (2006).
- [11] P. Horsch *et al.*, *Phys. Rev. Lett.* **94**, 076403 (2005).
- [12] M. Sofin, E.-M. Peters, and M. Jansen, *J. Solid State Chem.* **178**, 3708 (2005).
- [13] K. Kudo *et al.*, *Phys. Rev. B* **71**, 104413 (2005).
- [14] R. Jackiw and C. Rebbi, *Phys. Rev. D* **13**, 3398 (1976).
- [15] M. Mayr and P. Horsch, *Phys. Rev. B* **73**, 195103 (2006).
- [16] B. Valenzuela, S. Fratini, and D. Baeriswyl, *Phys. Rev. B* **68**, 045112 (2003), S. Fratini, B. Valenzuela, and D. Baeriswyl, *Synthetic Metals* **141**, 194 (2004).
- [17] As we treat rings with length L , our interaction is in fact $V_l = \max(V/l, V/(L-l))$, with $l_{\max} = L/2$.
- [18] As long as t_2 is not large enough to trigger the transition to the $\pi/2$ -CDW.
- [19] For truncated interaction ($l_{\max} = 3$) one finds $E_1 = 0.833$, $E_\infty = 1$, while for long-range Coulomb interaction we take $E_1 = \ln 2$, $E_\infty = 0.5$.